Lithium depletion in the Sun

P. Morel[1,3], J. Provost[1,3], G. Berthomieu[1,3],
J. Matias[2,3], J.P. Zahn[2,3]

[1]Département Cassini, URA CNRS 1362, Observatoire de la Côte d'Azur, France
[2]DASGAL, URA CNRS 335, Observatoire de Paris, France
[3]GDR, CNRS G131, Observatoire de Paris, France

Abstract: Physical properties of non-standard solar models including pre-main sequence phase, penetrative convection and microscopic diffusion are presented. We emphasize on ^{7}Li depletion.

1 Introduction

The observed abundance of ^{7}Li in the solar photosphere (Anders & Grevesse, 1989) corresponds to a depletion greater, by two orders of magnitude, of the value predicted by the standard Solar Models (sSM). ^{7}Li is destroyed at temperature greater than $2.6\,10^6$K. In sSM the most part of the ^{7}Li depletion occurs around the Zero Age Main Sequence (ZAMS) *i.e.* at the end of the Pre-Main Sequence (PMS) when the energy output, due to thermonuclear reactions, begins to overcome the release of gravitational energy. At that time the young Sun is fully convective and the depletion is due to the very effective convective mixing since ^{7}Li is only destroyed in the core. Though the microscopic diffusion sinks ^{7}Li towards regions of high temperatures, the depletion predicted by non sSM including microscopic diffusion (nsSMd) remains too small at the present solar age (Chaboyer *et al.*, 1992). It is known that the convective motions do not stop at the Schwarzschild limit but penetrate in the radiative zone. A consequence, for solar models, is an extent towards the lithium destruction regions of the adiabatic and chemically homogeneous zone (Zahn, 1991) and a concomitant increase of ^{7}Li depletion. PMS evolution, microscopic diffusion and penetrative convection then contribute to the ^{7}Li depletion. Hereafter we try to estimate the relative importance of these three processes.

2 Physics used in solar models

The solar models have been calculated using the CEFF equation of state – *i.e.* the EFF (Eggleton *et al.*, 1971) formalism with the Coulomb corrections – and the OPAL opacities (Rogers & Iglesias, 1992) extended by Kurucz's (1991b) opacities at low temperatures. The evolution is initialized by a PMS cold homogeneous convective model. Along the evolution, the atmosphere is restored using a set of $T(\tau, g)$ laws, derived from atmosphere models calculated with Kurucz's (1991a) ATLAS9 code. The bottom of the atmosphere is located at $\tau_{\rm Ross} = 20$. The radius of

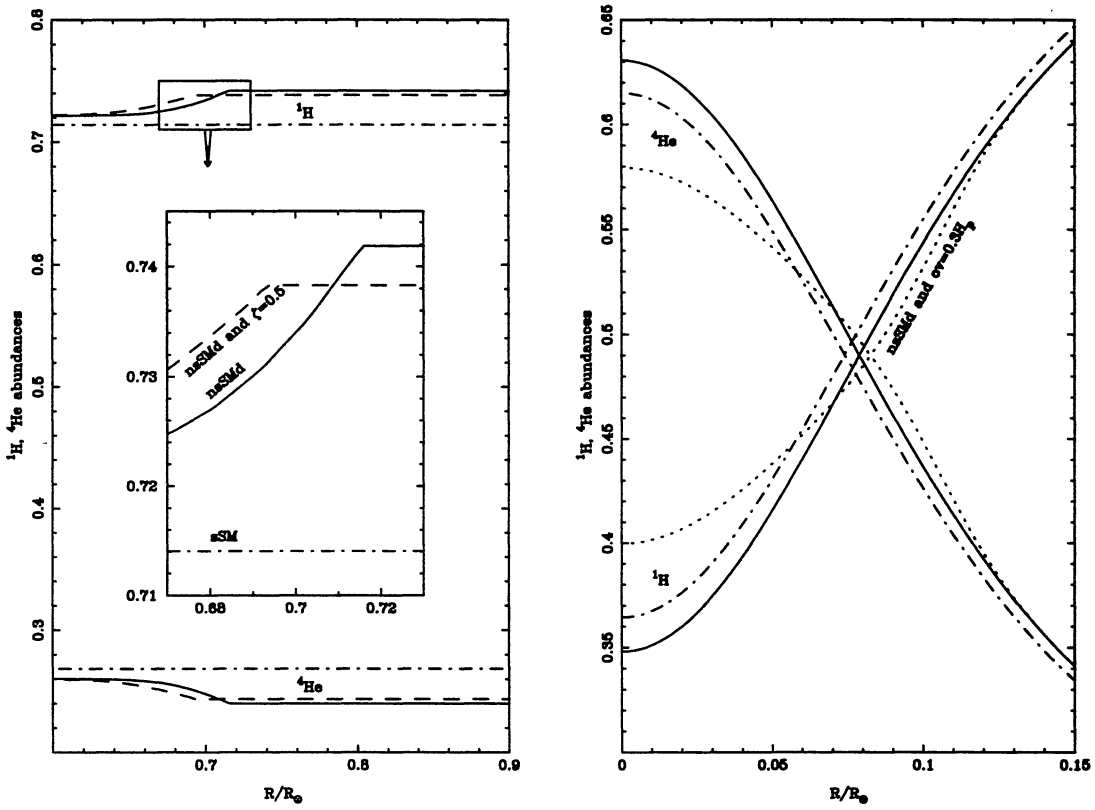

Figure 1: ^{1}H and ^{4}He profiles are plotted with respect to $R/R_\odot$ for standard Solar Model (sSM, dash-dot-dash), no sSM with microscopic diffusion (nsSMd, full), nsSMd with convective penetration $\zeta = 0.5$ (nsSMdζ, dashed), nsSMd and overshooting of the convective core of $0.3H_p$ (nsSMdo, dotted). **Left:** the neighbourhood of the bottom of the convective zone. The penetrative convection enlarged the mixed zone. That leads to a larger depletion of ^{1}H in nsSMdζ than in nsSMd and the reverse for ^{4}He. **Right:** the vicinity of the center. Due to its drag towards the surface, the ^{1}H abundance is lower in nsSMd than in sSM. For nsSMdo, a convective core is present up to ~3Gy, due to the mixing, the ^{1}H abundance is larger than in the other models.

the model is defined at the *variable* optical depth $\tau_\star(T_{eff}, g)$ defined by $T(\tau_\star) = T_{\rm eff}$ (Morel *et al.*, 1994). Therefore $\tau_\star$, as a function of T_{eff} and g, varies with time. In some models an overshoot of the young Sun convective core is allowed to an extent of $L_{\rm ov} = \lambda \min(R_{\rm core}, H_{\rm p})$, here $R_{\rm core}$ is the radius of the convective core, $H_{\rm p}$ is the pressure scale hight and λ is a free parameter, $0 \leq \lambda \lessapprox 0.3$. The enlargement of convective zones by convective penetration, $L_{\rm p} = \zeta \frac{H_p}{\chi_p}$, (Zahn, 1991) is characterized by ζ, $0 \leq \zeta \lessapprox 0.5$ with $\chi_p = \left(\frac{\partial \ln \chi}{\partial \ln P}\right)_{\rm ad}$ and $\chi = \frac{16\sigma T^4}{3\kappa\rho}$. For the Sun $L_{\rm p}$ is roughly $\sim \frac{\zeta}{1.8} H_{\rm p}$. The microscopic diffusion coefficients, for the chemical species ^{1}H, ^{2}D, ^{3}He, ^{4}He, ^{7}Li, ^{7}Be, ^{12}C, ^{13}C, ^{14}N, ^{15}N, ^{16}O and ^{17}O, are calculated using the formulations of Michaud & Proffitt (1993). In their formulation, the diffusion velocities are given for a mixture of fully ionized ^{1}H and ^{4}He, while the other elements, present in small amount, are considered as tracing elements. In convective zones, possibly extended by penetrative convection or overshooting, a quasi-instantaneous mixing, with a time scale of $\sim$ 15 years, is made by strong turbulent diffusion. The diffusion equation and the nuclear reactions involved by the PP and the CNO cycles using the above 12 chemical species are solved simultaneously. Equilibrium is not assumed for none of the elements. Weak screening is used. The reaction rates are taken from the tabulations of Caughlan & Fowler (1988). The initial abundances are the meteoritic values of Anders & Grevesse (1989). The solar models are calibrated, with a relative accuracy of 10^{-4}, by adjusting the mixing length parameter, the helium initial abundance ^{4}He$_i$ and the initial mass ratio $(Z/X)_i$ of heavy elements to hydrogen, in order that the model has, after $t_\odot = 4.55$ Gy of evolution, a radius $R_\odot = 6.9599\,10^{10}$ cm, a luminosity $L_\odot = 3.846\,10^{33}$ erg s^{-1} and, in the photosphere, $(Z/X)_\odot = 0.0245$. The characteristic low degree p-mode frequencies differences $\delta\nu_{02}$ and $\delta\nu_{13}$ are calculated according to Berthomieu *et al.*(1993).

3 Results and discussion

The microscopic diffusion (Fig. 1) drags ^{1}H to the surface and sinks the other elements to the center. In nsSMd, the photospheric helium abundance ^{4}He$_\odot$, the radius of the bottom of the convective zone R_ζ and $\delta\nu_{02}$ and $\delta\nu_{13}$ (Table 1, model nSMd) are very close the observations, that is a significant improvement with respect to sSM. On the other hand, the abundance of ^{7}Li remains very far from its observed value and the neutrinos fluxes are higher than in sSM. The depletion of ^{1}H in the vicinity of the center (Fig. 1, right) decreases the available nuclear fuel leading, via the calibration process, to an increase of the central temperature and to a concomitant increase of the neutrinos fluxes. The convective penetration deepen the bottom of the mixed region, as seen from Table 1, the value $\zeta \sim 0.5$ appears to be too large since the radius of the bottom of the mixed region is far below the value obtained by helioseismology. Nevertheless, even with this *(too large)* amount of penetrative convection, the ^{7}Li depletion is not important along the main sequence and almost constant whatever the amount of penetrative convection is. That means that the drag of ^{7}Li, due to the microscopic diffusion is not efficient enough . On the other hand, the ^{7}Li depletion occurs mainly during the PMS (Fig. 2 and Fig. 3). The greater ζ is, the higher will be ^{7}Li depletion.

At the end of the PMS the young Sun, between $\sim$ 1My and $\sim$ 80My presents a convective core which extends up to $\lessapprox 0.1 R_\odot$. The mixing in this convective core delays the depletion of ^{1}H due to the microscopic diffusion. This delay is increased if an overshoot of the convective core is allowed for. The larger the overshoot is, the longer will last the convective core, the lower will be the central temperature and the neutrino fluxes. With a *large* overshoot of $0.3 H_{\rm p}$, the convective core is present until 3Gy but without a significant effect on the neutrinos fluxes.

		$\odot$	SM	nSMd	nsSMdζ	nsSMdζ	nsSMdζ	nsSMdo
l/H_p			1.77	2.01	2.00	2.00	2.00	2.00
ζ			0	0	0.1	0.3	0.5	0
λ			0	0	0	0	0	0.3
^4He_i			0.269	0.270	0.270	0.270	0.270	0.271
$(\frac{Z}{X})_i$			0.0245	0.0255	0.0255	0.0254	0.0254	0.0255
$\delta\nu_{02}$	μHz	9.3	9.46	9.14	9.17	9.18	9.17	9.18
$\delta\nu_{13}$	μHz	16.5	16.44	16.07	16.06	16.05	16.06	16.66
$^4He_\odot$		0.242	0.269	0.240	0.241	0.242	0.244	0.240
^7Li_Z	dex		3.33	3.20	3.11	2.82	2.36	3.20
$^7Li_\odot$	dex	1.12	3.32	3.13	3.04	2.74	2.27	3.13
R_ζ	$R_\odot$	0.713	0.733	0.716	0.711	0.702	0.693	0.716
Φ_{Ga}	snu	79	121	126	126	126	126	127
Φ_{Cl}	snu	2.55	6.29	7.27	7.17	7.22	7.21	7.46
Φ_{Ka}	ev/d	0.28	0.48	0.57	0.56	0.57	0.56	0.59
T_c	10^6K		15.38	15.52	15.51	15.51	15.51	15.53
ρ_c	gr cm^{-3}		148	152	152	152	152	141
^1H_c			0.364	0.348	0.349	0.349	0.349	0.400

Table 1: Observations ($\odot$) and characteristics of the solar models of Fig. 1. Φ_{Ga}, Φ_{Cl}, Φ_{Ka} are the neutrino fluxes respectively for gallium, chlorine and Kamiokande experiments. ^7Li_Z and $^7Li_\odot$ are the ^{7}Li abundances at ZAMS and at present time. R_ζ is the radius, in solar unit, of the bottom of the mixed zone.

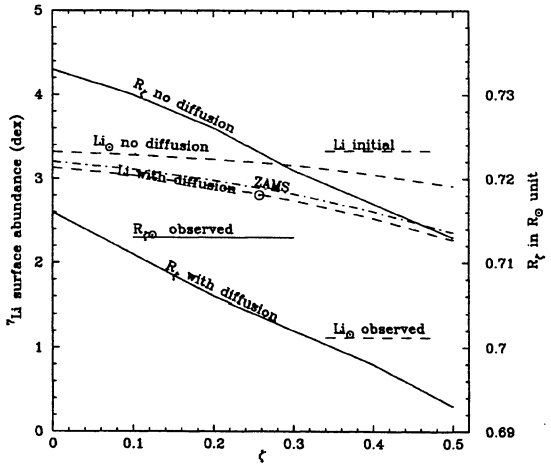

Figure 2: The ^{7}Li abundance and R_ζ are plotted with respect to ζ. The ^{7}Li depletion during the main sequence is constant whatever ζ is. The most part of the depletion occurs during the PMS. With $\zeta = 0.5$ the microscopic diffusion is not able to lower the ^{7}Li abundance to its observed value while R_ζ is significantly deeper than the observed value.

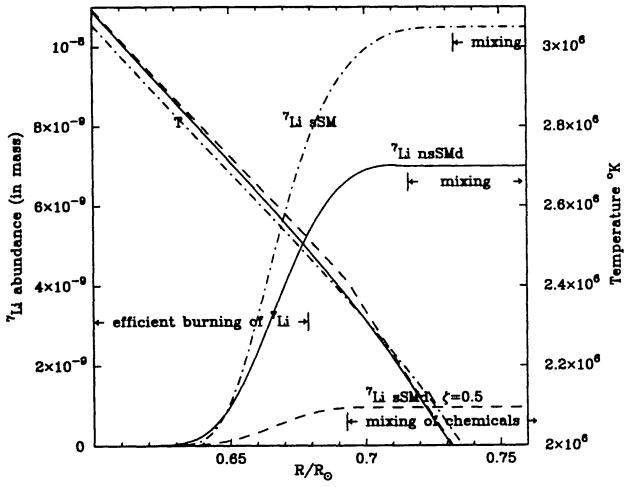

Figure 3: The external zone of ^{7}Li burning. The microscopic diffusion sinks ^{7}Li towards regions of temperature greater than 2.6 10^6K, there ^{7}Li is destroyed. The larger the mixed region is, the larger will be ^{7}Li depletion.

4 Conclusion

Neither the PMS phase, nor the microscopic diffusion, nor the penetrative convection, generate a ^{7}Li depletion close to the observations. The high ^{7}Li depletion observed in the Sun is, perhaps, due to some physical processes ignored in this work as the macroscopic diffusion and/or the rotation.

References

Anders, E., Grevesse, N., 1989, *Geochimica et Cosmochimica Acta*, **53**, 197

Berthomieu, G., Provost, J., Morel, P., Lebreton, Y., 1993, *A&A*, **268**, 775

Caughlan, G.R., Fowler, W.A., 1988, *Atomic Data and Nuclear Data Tables*, **40**, 284

Chaboyer, B.C., Deliyannis, C.P., Demarque, P., Pinsonneault, M.H., Sarajedini, A., 1992, *ApJ*, **348**, 372

Eggleton, P.P., Faulkner, J., Flannery, B.P. 1973, *A&A*, **23**, 325

Kurucz, R.L., 1991a, *Precision Photometry: Astrophysics of the Galaxy*, A.G. Davis, A.G. Philips, A.R. Upgren and K.A. Janes (eds.), L. Davis Press, Shenectady

Kurucz, R.L., 1991b, *Stellar Atmospheres: Beyond Classical Models*, L.Crivellari, I. Hubeny, and D.G. Hummer (eds), NATO ASI Series, Kluwer, Dordrecht, 1991

Michaud, G., Proffitt, C.R., 1993, *Inside the Stars*, IAU colloquium 137, ASP Conf. Ser., **40**, Weiss W.W. and Baglin A. (eds.), p. 247

Morel, P., van't Veer, C., Berthomieu, G., Castelli, F., Cayrel, R., Lebreton, Y., Provost, J., 1994, *A&A*, **286**, 91

Rogers, F.J., Iglesias, C.A., 1992, *ApJS*, **79**, 507

Zahn, J.P., 1991, *A&A*, **252**, 179